Probe Studies of the MgADP State of Muscle Cross-Bridges: Microscopic and Wavelength-Dependent Fluorescence Polarization from 1,5-IAEDANS-Labeled Myosin Subfragment 1 Decorating Muscle Fibers†

Katalin Ajtai‡ and Thomas P. Burghardt*

Cardiovascular Research Institute, University of California, San Francisco, San Francisco, California 94143-0524

Received October 10, 1986; Revised Manuscript Received January 14, 1987

ABSTRACT: The microscopic and wavelength-dependent fluorescence polarization signals from the 5-[[[(iodoacetyl)amino]ethyl]amino]naphthalene-1-sulfonic acid (1,5-IAEDANS) labeled subfragment 1 of myosin (S-1) decorating muscle fibers in rigor and in the presence of MgADP are measured. Using microscopic fluorescence polarization, we select a small uniform volume ($\sim$0.1 μm^3) from the muscle fiber and detect a high degree of angular order. From these data we show that the probe angular distribution from fibers in rigor is quantitatively different from that present when MgADP is bound to S-1. Using wavelength-dependent fluorescence polarization, we vary the wavelength of the excitation light and thereby change the direction that the probe absorption dipole makes with a reference frame fixed in S-1. From these data we show that the binding of MgADP to S-1 causes an angular reorientation of S-1 relative to the actin filament. The difference between the angular distribution of probes for the rigor vs. MgADP states cannot be accounted for by the addition of random probes. The microscopic fluorescence polarization experiments suggest that the earlier attempts to distinguish a rigor from a MgADP probe angular distribution by using the 1,5-IAEDANS probe failed due to the lower resolution of the optical technique employed. The wavelength-dependent fluorescence polarization experiments indicate that the probe dipole orientation on S-1, at the typically used excitation and emission wavelengths, is not ideal for detecting the orientation change in the rigor to MgADP angular transition.

Fluorescent probe studies established the ability of the myosin cross-bridge to bind to the actin filament at more than one orientation. Previously, we showed (iodoacetyl)tetramethylrhodamine (IATR), covalently linked to the SH_1 thiol of myosin, undergoes a large angular displacement from its rigor orientation when the cross-bridge binds MgADP (Borejdo et al., 1982; Burghardt et al., 1983; Ajtai & Burghardt, 1986) and when the cross-bridge is at low temperature in the presence of glycerol (Ajtai & Burghardt, 1986). Other probes, most notably 1,5-IAEDANS[1] (Borejdo et al., 1982) and spin probes (Thomas & Cooke, 1980) also linked to SH_1, showed no angular reorientation upon the binding of MgADP. The conflicting findings suggested the probes have different orientations relative to the molecular frame of the cross-bridge so that the rhodamine probe resides on the cross-bridge at an angle favorable to detecting cross-bridge angular displacement while 1,5-IAEDANS and spin probes maintain an unfavorable angle (Burghardt & Ajtai, 1985). Here we investigate this possibility for the 1,5-IAEDANS probe.

We measure microscopic fluorescence polarization and wavelength-dependent fluorescence polarization from 1,5-IAEDANS-labeled subfragment 1 (S-1) decorating glycerinated muscle fibers to investigate the angular distribution of probes in rigor and in the presence of MgADP. With microscopic fluorescence polarization we focus a linearly polarized laser beam to a very small volume ($\sim$0.1 μm^3) in a decorated muscle fiber, using a high numerical aperture objective. The small volume that is illuminated defines a uniform fiber sample. The fluorescence polarization measurements show that the probe on S-1 maintains distinct angular distributions relative to the actin filament for the rigor and MgADP states. We indicate the qualitative shape of the two angular distributions, using the formalism of model-independent fluorescence polarization (Burghardt, 1984).

With wavelength-dependent fluorescence polarization we demonstrate, using the wavelength dependence of the absorption dipole orientation relative to a reference frame fixed in S-1, that there is a dipole orientation for which the binding of MgADP to S-1 is observed to cause an unambiguous angular transition of the probe on S-1. This angular transition is unambiguous because it cannot be explained by increasing probe disorder but only by a probe reorientation upon the binding of MgADP.

Control experiments indicate that the local environment of the probe and the shape of S-1 are not perturbed by the binding of MgADP to S-1 so that the microscopic and wavelength-dependent fluorescence polarization results are interpreted as S-1 undergoing reorientation upon the binding of MgADP. The microscopic experiments permit fluorescence polarization to be applied to a uniform fiber sample. Previously, a lower resolution microscopic optical technique failed to distinguish the MgADP from the rigor state, using the 1,5-IAEDANS probe. The present results suggest the previous attempt failed due to the lower angular resolution of the

† This work was supported by U.S. Public Health Service Grant HL-16683 and by the Muscular Dystrophy Association.

* Address correspondence to this author at the Department of Biochemistry and Molecular Biology, Mayo Foundation, Rochester, MN 55905.

‡ Present address: Department of Biochemistry and Molecular Biology, Mayo Foundation, Rochester, MN 55905, and Department of Biochemistry, Eötvös Loránd University, Budapest, Hungary.

[1] Abbreviations: EGTA, ethylene glycol bis(β-aminoethyl ether)-*N*,*N*,*N*′,*N*′-tetraacetic acid; ESR, electron spin resonance; 1,5-IAEDANS, 5-[[[(iodoacetyl)amino]ethyl]amino]naphthalene-1-sulfonic acid; S-1, myosin subfragment 1; SDS–PAGE, sodium dodecyl sulfate–polyacrylamide gel electrophoresis.

0006-2960/87/0426-4517$01.50/0

microscopic linear dichroism technique (Borejdo et al., 1982). The wavelength-dependent experiments strongly support the suggestion that the earlier conflicting result for the two fluorescent probes was due to differing probe dipole orientations relative to S-1.

We have also performed microscopic fluorescence polarization measurements on 1,5-IAEDANS-labeled split S-1 decorating muscle fibers. We found the probe angular distribution for split S-1 in rigor is distinct from native S-1 in rigor and resembles that of native S-1 in the presence of MgADP. The probe angular distribution in the presence of MgADP is unaffected by the splitting of S-1. These results show that the cutting of S-1 alters its structure in a manner similar to that caused by the binding of MgADP when S-1 is actin bound.

Materials and Methods

Materials

Chemicals. ATP, ADP, P^1,P^5-bis(5′-adenosyl) pentaphosphate (Ap_5A), and hexokinase were from Sigma (St. Louis, MO). 1,5-IAEDANS was from Molecular Probes (Eugene, OR). All chemicals were of analytical grade.

Solutions. Rigor solution contained 80 mM KCl, 5 mM $MgCl_2$, 2 mM EGTA, 5 mM sodium phosphate, and 1 mM dithiothreitol at pH 7.0. Relaxing solution was rigor solution was 4 mM ATP. ADP containing solution was rigor solution with 4 mM ADP, 10 μM glucose, and 100 μg/mL hexokinase to remove contaminating ATP and 100 μM Ap_5A to inhibit myofibrillar myokinase from converting ADP to ATP.

Proteins. Rabbit myosin was prepared by a standard method (Tonomura et al., 1966); α-chymotrypsin digested myosin filaments in the S-1 preparation (Weeds & Taylor, 1975). The labeling of S-1 with 1,5-IAEDANS was carried out as described by Duke et al. (1976).

Preparation of Split S-1. 1,5-IAEDANS-labeled S-1 at a concentration of 1 mg/mL was digested in rigor solution for 30 min at 25 °C. The molar ratio of trypsin to S-1 was 1:80. Soybean inhibitor at a ratio of 1:2 trypsin to inhibitor stopped the reaction. The peptide composition of the digest was analyzed by SDS–PAGE and showed that the heavy chain of S-1 was cleaved into the usual fragments of molecular weights 27K, 50K, and 20K.

Muscle Fibers. We obtained rabbit psoas muscle fibers as described previously (Borejdo et al., 1979) and kept them in a relaxing + 50% glycerol (1:1 relax to glycerol by volume, pH 7.0) solution at −15 °C for up to several weeks. Single fibers at rest length were washed in rigor solution and transferred to the quartz slide or mounted on the rectangular stainless steel support. The decoration of the fibers with 1,5-IAEDANS-labeled native or split S-1 was done in rigor at 4 °C with a protein concentration of 1 mg/mL for 15–30 min. Washing with rigor or MgADP-containing solution immediately before an experiment removed unbound labeled protein. We observed that it was not necessary to wash out the unbound protein in the microscopic experiments since its presence did not affect the fluorescence polarization results. This is due to the high affinity of S-1 for actin in the fiber and the small depth of focus of the objective used with an image plane diaphragm.

Fiber quality was assessed in two ways. First, the fibers were inspected for uniform shape and normal appearance in the dissecting microscope just prior to decoration with S-1. Second, $P_\parallel$ from the decorated fibers was measured at standard wavelengths (λ_{ex} = 370 nm; λ_{em} = 410 nm). Decorated fibers with $P_\parallel < 0.5$ were rejected as too disordered. In the microscopic experiments the uniformity of the single fiber sample was observed under the microscope at high magnification. Fiber regions chosen for experimentation were uniform and parallel to the parallel polarization of the excitation light. With these select fibers all of the observable effects induced by the presence of MgADP were reversible (by removing MgADP).

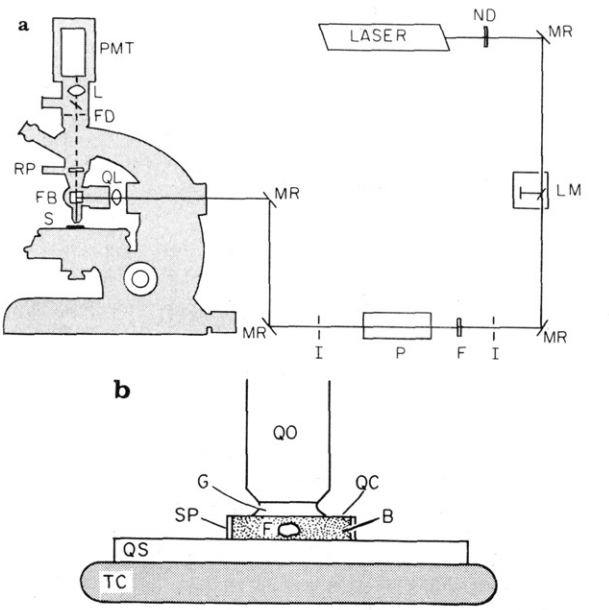

FIGURE 1: Microscopic fluorescence polarization apparatus (a). A neutral density filter (ND) attenuates the 364-nm line from an argon ion laser that is reflected by several UV reflecting mirrors (MR). A photodiode monitors the laser intensity (LM) and normalizes the fluorescence signal. Iris diaphragms (I) position the beam through the Pockels Cell (P) that rotates the beam polarization. A quartz lens (QL) focuses the laser beam at the back focal plane of the quartz objective. The objective focuses the beam on the sample (S). A dichroic mirror in the filter block (FB) reflects the excitation beam and transmits the longer wavelength fluorescence from the sample. A rotating film polarizer (RP) analyzes the fluorescence for polarization. The field diaphragm (FD) in the image plane of the microscope is adjusted to be just larger than the image of the focused spot on the sample to exclude out-of-focus fluorescence and stray light. Fluorescence intensity through the field diaphragm is focused by a lens (L) onto the photocathode of the photomultiplier (PMT). The microscope stage (b). The quartz objective (QO) focuses the laser beam onto the muscle fiber (F) bathed in a buffer (B). The buffer is maintained between spacers (SP), a quartz slide (QS), and a quartz cover slip (QC). The objective immersion fluid is glycerol (G). A temperature-controlled microscope stage (TC) holds the temperature of the fiber constant.

All experiments were performed at 20 °C except where noted otherwise.

Methods

Microscopic Fluorescence Polarization. A quartz lens focuses an argon laser beam (λ_0 = 364 nm; Spectra Physics) on the back image plane of an epi-illumination fluorescence microscope (Zeiss Photomicroscope III); see Figure 1a. The high-aperture quartz objective (Zeiss; NA = 1.25, glycerine immersion) focuses the beam to a small volume (~0.1 μm^3) in the muscle fiber that is mounted on a quartz slide and covered by a quartz cover slip (Heraeus-Amersil, Sayreville, NJ); see Figure 1b.

A Pockels Cell, driven by a broad bandwidth amplifier (Lasermetrics Inc., Englewood, NJ), controls the polarization of the laser beam. The amplifier is interfaced to an Eclipse S/230 computer (Data General Corp., Westboro, MA). The beam polarization rotates through 90° from parallel to perpendicular to the fiber axis every 5 ms. During each 5-ms interval the microscope objective collects the fluorescence

emission and a photomultiplier tube (Hamamatsu R1332) detects single photons. The single-photon pulses are amplified, discriminated, and counted in one of two scalar channels in a CAMAC Quad Scalar controlled by the Eclipse. One channel is dedicated to emission resulting from parallel excitation, and the other is dedicated to perpendicular excitation. The real time clock of the Eclipse starts an experiment every 10 ms, and a custom-made circuit (M. Bilk, Inc., San Francisco, CA) directs the discriminated pulses to the correct CAMAC scalar. The Eclipse reads and resets the scalars after each 10-ms experiment and displays the average intensities every second.

The filter block (Figure 1a) contains a dichroic mirror and a barrier filter. The dichroic mirror reflects the excitation light through the objective and transmits the longer wavelength fluorescence (cutoff at 420 nm) collected by the objective. A rotatable film polarizer analyzes the fluorescence. A lens focuses the fluorescence at an image plane diaphragm that admits light only from the fluorophores excited by the focused laser beam. A complete experiment takes ~5 s to perform.

We describe elsewhere the optical correction for the quartz cover slip and the high-aperture light collection of the objective when fluorescence polarization is measured (Burghardt & Thompson, 1984). The results below are corrected for these effects.

Wavelength-Dependent Fluorescence Polarization. The wavelength-dependent experiments were performed on a SLM 8000 spectrofluorometer (SLM Instruments, Urbana, IL) equipped with Glan-Thompson polarizers. A 1.4 × 3.0 cm rectangular stainless steel support, made to fit inside a standard fluorescence cuvette, held mounted fibers in the excitation beam path (Burghardt & Ajtai, 1985). The emission was collected at 90° from the excitation beam path at emission wavelengths >500 nm with a cutoff filter. We oriented the fiber such that the fiber axis was perpendicular to the plane defined by the path of the excitation and collected emission beams.

The illuminated volume in this instrument is ~1 mm^3.

Lifetime Measurements. Lifetime measurements on 1,5-IAEDANS-labeled S-1 decorating fibers in rigor and in the presence of MgADP were performed on an instrument described earlier (Torgerson & Morales, 1984). We mounted fibers in the same manner as in the wavelength-dependent experiments.

An interference filter with a bandwidth of 10 nm centered the wavelength of the excitation light at 350 nm. Emission was collected at wavelengths >440 nm with a cutoff filter.

Data Analysis. The order parameters $a^j_{m,n}$ describe the probe angular distribution $N(\Omega)$ with the relation (Burghardt, 1984)

$$N(\Omega) = \sum_{j=0}^{\infty}\sum_{m,n=-j}^{j}\sqrt{(2j+1)/(8\pi^2)}\,a^j_{m,n}D^j_{m,n}(\Omega) \quad (1)$$

where Ω stands for the three Euler angles α, β, and γ describing the orientation of a molecular reference frame fixed inside the cross-bridge and $D^j_{m,n}(\Omega)$ is an element of the Wigner rotation matrix (Davydov, 1963).

Known properties of the muscle fiber and a particular choice of the molecular coordinate frame greatly simplify eq 1. There is experimental evidence indicating that a muscle fiber has azimuthal symmetry such that it is unchanged by an arbitrary rotation about the fiber axis (Burghardt et al., 1983). If the fiber axis is placed along the lab frame z axis, then α is the independent variable for the probe angular distribution about the fiber axis and azimuthal symmetry in the fiber requires $N(\Omega)$ be independent of α. This fact is expressed implicitly in $N(\Omega)$ by requiring $a^j_{m,n} = a^j_{0,n}\delta_{m,0}$, where $\delta_{m,0}$ is the Kronecker δ, in eq 1. It is well-known that a 180° rotation relates opposite half-sarcomeres in a muscle fiber. This symmetry property requires $a^j_{0,n} = 0$ unless $j - n = 0, 2, 4, \ldots$. Furthermore, we choose to express the probe angular distribution relative to a molecular coordinate frame wherein the absorption dipole μ_a points along the z axis and the xy projection of the emission dipole μ_e points along the x axis. This choice of molecular coordinate frames makes β the polar degree of freedom and γ the torsional degree of freedom of the molecular coordinate frame and renders the fluorescence polarization signal independent of order parameters $a^j_{0,n}$ except when $n = 0$ or ± 2 (inspection of eq 17 in Burghardt (1984) verifies this result). This last restriction on index n is not a result of fiber symmetry but of the properties of dipolar emission.

The theoretical fluorescence intensity $F(\psi, \chi)$ for emission collection collinear with excitation (as in Figure 1a) is expressed in terms of order parameters by (Burghardt, 1984)

$$F(\psi,\chi)/F_0 = (1/9)(K_a + K_b + K_c) + \sum_{j=0}^{4}\sum_{n=-j}^{j}\sqrt{8\pi^2/(2j+1)}\,a^j_{0,n}\{(1/3)f_0 m^a_n\delta_{j,2} + (1/3)b_0 m^e_n\delta_{j,2} + d^j_0 M^j_n\} \quad (2)$$

where F_0 is a constant, K_a, K_b, and K_c are the polarization correction factors for high-aperture collection of polarized light (Burghardt & Thompson, 1984), and

$$f_0 = \sqrt{2/3}(K_a + K_b + K_c)[\cos^2\psi - (1/2)\sin^2\psi] \quad (3a)$$

$$b_0 = \sqrt{2/3}[[K_c - (1/2)K_b]\cos^2\chi + [K_b - (1/2)K_c]\sin^2\chi - (1/2)K_a] \quad (3b)$$

$$d^j_0 = (1/2)\langle 2, 2, -2, 2|j, 0\rangle \sin^2\psi[K_c\sin^2\chi + K_b\cos^2\chi - K_a] + (2/3)\langle 2, 2, 0, 0|j, 0\rangle[\cos^2\psi - (1/2)\sin^2\psi][[K_c - (1/2)K_b]\cos^2\chi + [K_b - (1/2)K_c]\sin^2\chi - (1/2)K_a] - (1/2)(K_c - K_b)\times \langle 2, 2, 1, -1|j, 0\rangle \sin 2\psi \sin 2\chi \quad (3c)$$

$$M^j_0 = (2/3)\sqrt{2/3}\langle 2, 2, 0, 0|j, 0\rangle[\cos^2\theta_e - (1/2)\sin^2\theta_e] \quad (3d)$$

$$M^j_{\pm 2} = \sqrt{1/6}\langle 2, 2, \mp 2, 0|j, \mp 2\rangle \sin^2\theta_e \quad (3e)$$

$$m^a_0 = \sqrt{2/3} \quad (3f)$$

$$m^e_0 = \sqrt{2/3}[\cos^2\theta_e - (1/2)\sin^2\theta_e] \quad (3g)$$

$$m^e_{\pm 2} = (1/2)\sin^2\theta_e \quad (3h)$$

The quantities $\langle j_1, j_2, m_1, m_2|j, m\rangle$ appearing in eq 3c–e are Clebsch–Gordon coefficients (Davydov, 1963), and the parameter θ_e in eq 3d–h is the polar angle of the emission dipole. All other quantities in the sum of eq 2 that are not explicitly mentioned in eq 3a–h are zero.

An experiment consists of the measurement of the four fluorescence intensities $F_{\parallel,\parallel}$, $F_{\parallel,\perp}$, $F_{\perp,\parallel}$, and $F_{\perp,\perp}$. The symbols $\parallel$ and $\perp$ mean parallel and perpendicular to the fiber axis. The first index on F refers to the polarization of the excitation light, and the second refers to the polarization of the emission light. The three ratios, defined in eq 4, combine these four intensities and are independent of an overall constant related to the light transmission efficiency of the collection optics. The

ratios are related to the order parameters, using eq 2 and 3 such that

$$P_{\parallel} = \frac{F_{\parallel,\parallel} - F_{\parallel,\perp}}{F_{\parallel,\parallel} + F_{\parallel,\perp}} = \frac{F(\psi = 0, \chi = 0) - F(\psi = 0, \chi = \pi/2)}{F(\psi = 0, \chi = 0) + F(\psi = 0, \chi = \pi/2)} \quad (4a)$$

$$P_{\perp} = \frac{F_{\perp,\perp} - F_{\perp,\parallel}}{F_{\perp,\perp} + F_{\perp,\parallel}} = \frac{F(\psi = \pi/2, \chi = \pi/2) - F(\psi = \pi/2, \chi = 0)}{F(\psi = \pi/2, \chi = \pi/2) + F(\psi = \pi/2, \chi = 0)} \quad (4b)$$

$$Q_{\parallel} = \frac{F_{\parallel,\parallel} - F_{\perp,\parallel}}{F_{\parallel,\parallel} + F_{\perp,\parallel}} = \frac{F(\psi = 0, \chi = 0) - F(\psi = \pi/2, \chi = 0)}{F(\psi = 0, \chi = 0) + F(\psi = \pi/2, \chi = 0)} \quad (4c)$$

For the present case, eq 4a–c are solved simultaneously, where the unknowns are $a^2_{0,0}$, $a^2_{0,2} + a^2_{0,-2}$, $a^4_{0,0}$, and $a^4_{0,2} + a^4_{0,-2}$. The normalization of the angular distribution (integrated over all orientations, it equals 1) gives $a^0_{0,0} = [1/(8\pi^2)]^{1/2}$. A symbolic manipulation program SMP (Inference Corp., Pasadena, CA) solves eq 4a–c symbolically.

The other independent parameters we must know to solve eq 4a–c are the optical correction factors K_a, K_b, and K_c (see eq 2 and 3) and the angle between the absorption and emission dipoles θ_e (see eq 3). The correction factors are computed from formulas derived previously [eq 20 in Burghardt and Thompson (1984)] and are $K_a = 0.209$, $K_b = 0.0123$, and $K_c = 0.669$ (for glycerine immersion quartz objective with NA = 1.25 and quartz interfaces). The angle between the absorption and emission dipoles was estimated by measuring $P_{\parallel}$ from 1,5-IAEDANS-labeled S-1 in a rigor + 50% glycerol (1:1 rigor to glycerol by volume, pH 7.0) solution cooled to −20 °C and solving eq 4a with $a^j_{m,n} = [1/(8\pi^2)]^{1/2}\delta_{j,0}\delta_{m,0}\delta_{n,0}$. We find, for the microscopic illumination system with laser excitation at λ_{ex} = 364 nm and emission filter block cutoff at 420 nm, that $\theta_e = 23.0 \pm 2.0°$.

The four unknown order parameters $a^2_{0,0}$, $a^4_{0,0}$, $a^2_{0,2} + a^2_{0,-2}$, and $a^4_{0,2} + a^4_{0,-2}$ are constrained by three equations (eq 4a–c). Using SMP to solve eq 4a–c for three of the unknown order parameters, given the polarization ratios and the values for θ_e, K_a, K_b, and K_c, it is possible to show that $a^2_{0,2} + a^2_{0,-2}$ and $a^4_{0,2} + a^4_{0,-2}$ do not strongly contribute to the fluorescence polarization signal. We can show that large changes (~100%) in $a^2_{0,2} + a^2_{0,-2}$ or $a^4_{0,2} + a^4_{0,-2}$ make small changes (~10%) in $a^2_{0,0}$ and $a^4_{0,0}$. This asymmetry in the importance of the order parameters to the fluorescence polarization signal is due to the small value of θ_e since when $\theta_e = 0$, eq 4a–c are strictly independent of $a^2_{0,2} + a^2_{0,-2}$ and $a^4_{0,2} + a^4_{0,-2}$. This fluorescence polarization signal is clearly not a practical means of measuring $a^2_{0,2} + a^2_{0,-2}$ or $a^4_{0,2} + a^4_{0,-2}$. Additionally, because there are four unknown order parameters but only three equations (eq 4a–c) to constrain them, we must supply at least one new constraint. We obtain the additional constraint from the model-independent analysis of ESR spectra (Burghardt & Thompson, 1985).

The fluorescence and ESR data are quantitated in terms of order parameters, but the values of the order parameters are not interchangeable because in these applications both sets of order parameters describe the probe angular distribution. The probe angular distribution derived from ESR data describes how the spin probe is oriented. Likewise, the probe distribution derived from fluorescence data describes how the fluorescent probe is oriented. A rotation can always be found to relate the two sets of order parameters such that (Burghardt, 1984)

$$a^j_{m,n}(\text{fluorescence}) = \sum_{k=-j}^{j} a^j_{m,k}(\text{ESR}) D^j_{n,k}(\Omega_1) \quad (5)$$

where Ω_1 represents the Euler angles α_1, β_1, and γ_1 describing the rotation from the spin probe fixed frame to the fluorophore fixed frame. Equation 5 transforms the order parameters calculated in the principal magnetic frame of the spin probe to the reference frame of the fluorescent probe (for example, our choice with the z axis along the absorption dipole and the x axis along the projection of the emission dipole in the xy plane). The azimuthal symmetry of the fiber again requires $a^j_{k,n}(\text{ESR}) = 0$ unless $k = 0$ so that eq 5 reduces to the expression

$$a^j_{0,n}(\text{fluorescence}) = \sum_{k=-j}^{j} a^j_{0,k}(\text{ESR}) D^j_{n,k}(\Omega_1) \quad (6)$$

We estimate the value of Ω_1 by initially guessing its value and then calculating $a^2_{0,2} + a^2_{0,-2}$ (fluorescence) and $a^4_{0,2} + a^4_{0,-2}$ (fluorescence) using eq 6 and known values for $a^j_{0,k}$ (ESR). We then solve eq 4a–c for $a^2_{0,0}$ and $a^4_{0,0}$ (fluorescence) and compare these values with the values of $a^2_{0,0}$ and $a^4_{0,0}$ (fluorescence) computed directly from eq 6 and $a^j_{0,k}$ (ESR). On the basis of this comparison an improved estimate of Ω_1 is made, and we repeat the above steps until the difference between the fluorescence order parameters computed by the two methods is minimized.

Preliminary results from ESR data suggest $a^2_{0,0}$ (ESR) = −0.0727, $a^4_{0,0}$ (ESR) = 0.0342, $a^2_{0,2} + a^2_{0,-2}$ (ESR) = 0.158, and $a^4_{0,2} + a^4_{0,-2}$ (ESR) = −0.094 for fibers in rigor and in the presence of MgADP (J. Belágyi, K. Ajtai, and T. P. Burghardt, unpublished observations). By the method outlined above, we estimate (α_1, β_1, γ_1) = (124°, 62°, 26°) or (58°, 62°, 156°) for fibers in rigor and (α_1, β_1, γ_1) = (108°, 74°, 33°) or (74°, 74°, 149°) for fibers in the presence of MgADP. No error estimate is presently available for the ESR order parameters (only two ESR spectra have been analyzed), so no error estimate is attempted for the fluorescence order parameters. Consequently, we regard order parameters estimated by using eq 6 as giving a qualitative description of the probe angular distribution.

We will summarize our order parameter results with a plot of $\mathcal{N}(\beta)$, the polar angular distribution derived from $N(\Omega)$ by integrating over Euler angles α and γ. We find

$$\mathcal{N}(\beta) = \int_0^{2\pi} d\alpha \int_0^{2\pi} d\gamma N(\alpha, \beta, \gamma) = (4\pi^2) \sum_{j=0}^{4} a^j_{0,0} \sqrt{(2j+1)/(8\pi^2)} P_j(\cos\beta) \quad (7)$$

where $P_j(\cos\beta)$ is a Legendre polynomial.

RESULTS

Time-Resolved Fluorescence Measurements. The lifetime of 1,5-IAEDANS-labeled S-1 decorating muscle fibers in rigor and in the presence of MgADP was measured to ascertain the effect of MgADP binding on the local environment of the probe. In agreement with previous studies on acto-S-1 (Mendelson et al., 1975), we found the probe had a single lifetime of 20.0 ± 0.1 ns in rigor and in the presence of MgADP. This result indicates no lifetime-altering change in the local environment of this SH_1-bound probe upon the binding of MgADP when S-1 is actin bound.

Table I: Microscopic Fluorescence Polarization Ratios for Native and Split 1,5-IAEDANS-Labeled S-1[a]

	rigor		MgADP	
	native	split	native	split
$P_\parallel$	0.455 ± 0.008	0.51 ± 0.01	0.522 ± 0.008	0.55 ± 0.01
$P_\perp$	−0.19 ± 0.01	−0.210 ± 0.008	−0.25 ± 0.01	−0.28 ± 0.01
$Q_\parallel$	0.367 ± 0.008	0.460 ± 0.006	0.40 ± 0.01	0.485 ± 0.004

[a] $P_\parallel$, $P_\perp$, and $Q_\parallel$ are defined in eq 4 and were measured on the instrument described in Figure 1. An average of three experiments on selected regions of single fibers were performed on eight (native) or three (split) independently prepared single fibers. Errors are standard error in the mean with n = 25 (native) or 9 (split).

Mendelson et al. (1975) have also measured the effect of nucleotides on the fluorescence depolarization of 1,5-IAEDANS-labeled S-1 in solution. They found no observable change in the amplitude and rate of the polarization relaxation for S-1 in rigor compared to that in the presence of MgADP. This result suggests that there is no significant deformation of the shape of S-1 upon the binding of MgADP and that it is unlikely that the effect of the binding of MgADP to S-1 is to distort the domain of S-1 that contains SH_1.

Earlier work with 1,5-IAEDANS-labeled split S-1, in the presence of F actin, showed the binding of the nucleotide to split S-1 had no effect on the probe lifetime (Botts et al., 1982). Splitting S-1 appears to cause no detectable change in the local environment of the probe at SH_1.

Botts et al. (1982) have also shown the binding MgADP to split S-1 does not alter the amplitude and rate of the polarization relaxation of split S-1 in solution. As in the measurements on native S-1, this result suggests that there is no significant deformation of the shape of split S-1 upon the binding of MgADP and that it is unlikely that MgADP distorts the domain of split S-1 containing SH_1.

Microscopic Fluorescence Polarization. The apparatus of Figure 1 was used to measure the intensity ratios defined by eq 4a–c. Table I summarizes the experimental values of the ratios. The ratios indicate a quantitative difference between probe angular distributions for fibers decorated with native S-1 in rigor and in the presence of MgADP. We used the formalism of model-independent fluorescence polarization (Burghardt, 1984), as described under Methods, to deduce the order parameters of the probe angular distribution for these two fiber states. From the simultaneous solution of eq 4a–c, and the additional constraints from ESR (see Methods), we obtain for rigor fibers

$$a^2_{0,0} = 0.058 \quad (8a)$$

$$a^2_{0,2} + a^2_{0,-2} = 0.056 \quad (8b)$$

$$a^4_{0,0} = -0.021 \quad (8c)$$

$$a^4_{0,2} + a^4_{0,-2} = 0.042 \quad (8d)$$

and for fibers in the presence of MgADP

$$a^2_{0,0} = 0.066 \quad (9a)$$

$$a^2_{0,2} + a^2_{0,-2} = 0.060 \quad (9b)$$

$$a^4_{0,0} = 0.0089 \quad (9c)$$

$$a^4_{0,2} + a^4_{0,-2} = 0.046 \quad (9d)$$

As described under Methods, the values of $a^2_{0,2} + a^2_{0,-2}$ and $a^4_{0,2} + a^4_{0,-2}$ appearing in eq 8 and 9 were obtained from eq 6 and the preliminary results from ESR data. Although the polarization ratios in Table I indicate a clear quantitative difference between the probe angular distributions for fibers decorated with native S-1 in rigor and in the presence of MgADP, we can make no similar conclusion from the order parameters. A reliable error estimate for the order parameters must await a reliable error estimate for order parameters derived from ESR spectra. We regard the order parameter values of eq 8 and 9 as a qualitative description of the probe angular distributions.

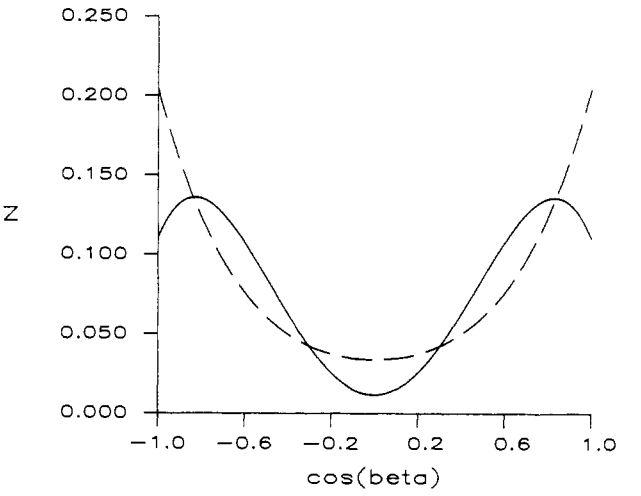

FIGURE 2: Probe polar angular distribution for 1,5-IAEDANS-labeled S-1 decorating muscle fibers in rigor (—) and in the presence of MgADP (– –). β is the polar probe angle. The distributions are normalized to have the same area.

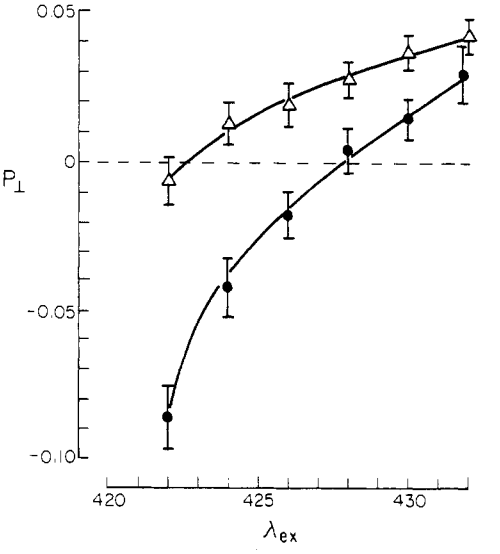

FIGURE 3: $P_\perp$ measured from 1,5-IAEDANS-labeled S-1 decorating muscle fibers in rigor (●) and in the presence of MgADP (△) as a function of excitation wavelength, λ_{ex}. λ_{ex} is measured in nanometers. Error bars indicate standard error of the mean with n = 6–8. A total of eight independent fiber preparations were used.

The values of $a^2_{0,0}$ and $a^4_{0,0}$ in eq 8 and 9 are used in eq 7 to plot $\mathcal{N}(\beta)$ for fibers in rigor and in the presence of MgADP in Figure 2. These plots indicate the qualitative relationship between the polar angular distributions for decorated fibers in rigor and in the presence of MgADP. The plots in Figure

2 are in good qualitative agreement with those obtained from preliminary studies of ESR spectra (J. Belágyi, K. Ajtai, and T. P. Burghardt, unpublished observations).

Wavelength-Dependent Fluorescence Polarization. $P_\perp$ as a function of excitation wavelength, λ_{ex}, for fibers in rigor and in the presence of MgADP, is shown in Figure 3. Figure 3 shows that, near $\lambda_{ex} = 426$ nm, fibers in rigor are characterized by $P_\perp < 0$ and in the presence of MgADP by $P_\perp > 0$. For a random distribution of probes, $P_\perp = 0$ at any wavelength. These data indicate that the probe angular distributions for these two states are unmistakably different since the addition of a random distribution to either probe distribution will not transform one distribution into the other. Clearly this observation rules out the unlikely possibility that the difference between rigor and MgADP probe angular distributions is a result of actin-dissociated S-1 in the sample region.

These data also indicate that near $\lambda_{ex} = 426$ nm the absorption dipoles for probes in rigor fibers are predominantly parallel to the fiber axis while the probes from fibers in the presence of MgADP are predominantly perpendicular to the fiber axis. The time-resolved fluorescence studies, indicating that there is no probe environment and no shape change in S-1 upon nucleotide binding, suggest that the binding of the nucleotide causes the cross-bridge to rotate from the rigor cross-bridge orientation.

Microscopic Studies of Split S-1. We studied the involvement of the domains of S-1 in the determination of the orientation distribution of the acto-S-1 attachment in different conditions, using 1,5-IAEDANS-labeled split S-1. The muscle fibers were decorated with the split S-1 and examined with microscopic fluorescence polarization. The results, summarized in Table I, show that the effect of the cut between the actin binding domains alters the probe orientation in the S-1 decoration. The probe orientation for split S-1 in rigor is more ordered and is similar to the probe orientation for native S-1 in the presence of MgADP. The probe orientation for split S-1 in MgADP is similar to the native S-1 orientation in MgADP.

Discussion

The identification of cross-bridge orientation in muscle fibers is a task well suited to fluorescent and ESR probe studies. The apparent disagreement of results from these techniques caused us to search for a verifiable explanation of this disagreement. In this paper we examine the results from the fluorescent probe 1,5-IAEDANS modifying SH_1 on S-1 decorated fibers. Previously, it was believed that 1,5-IAEDANS revealed no effect on the rigor probe angular distribution upon the binding of MgADP to the cross-bridge (Borejdo et al., 1982). Here we show that microscopic fluorescence polarization detects significant changes in the polarization ratios $P_\parallel$, $P_\perp$, and $Q_\parallel$ (see Table I), suggesting that a reorientation of the S-1 occurs. The reorientation is qualitatively represented by the probe polar angular distribution of Figure 2.

The difference in the qualitative probe orientation distributions indicated in Figure 2 indicates a rigor cross-bridge rotation upon the binding of MgADP. The rotating cross-bridge model of muscle contraction holds that the active cross-bridge rotates while attached to actin to produce fiber shortening. Thus it is important to verify quantitatively if the cross-bridge rotates. We verify that the cross-bridge reorients upon the binding of MgADP, using the directional dependence of the 1,5-IAEDANS absorption dipole moment on excitation wavelength (Hudson & Weber, 1973). We show in Figure 3 that $P_\perp < 0$ for the rigor cross-bridge and $P_\perp > 0$ for the cross-bridge in the presence of MgADP. Because the local environment of the probe on S-1 and the domain in S-1 containing the probe are probably not perturbed by the binding of MgADP, it is unlikely that the observed inequalities for $P_\perp$ can be satisfied without cross-bridge rotation. This conclusion depends ultimately on the indication of no local probe movement when acto-S-1 binds MgADP from the time-resolved fluorescence experiments. It is conceivable that a local probe rotation occurs that does not alter its environment and does not change the probe's orientation relative to the principal hydrodynamic frame of S-1. Our observations, however, strongly suggest that the distinctive probe orientation distributions obtained for rigor vs. MgADP cross-bridges can only be explained by a cross-bridge reorientation upon the binding of MgADP.

We conclude that fluorescence probes, excluding fluorescent nucleotides with which it is impossible to achieve the rigor state (Yanagida, 1981, 1985), distinguish the orientation distribution of the rigor and MgADP states of the cross-bridges (Borejdo et al., 1982). The preponderance of fluorescent probe data now agrees that the rigor and the MgADP states of the fiber are distinct.

The results of the split S-1 decoration experiments show that the split protein undergoes a structural change that alters the angular distribution of probes in rigor. The split S-1 angular distribution in rigor resembles that of native S-1 in the presence of MgADP (see Table I). This finding could be important for the interpretation of the cross-linking results between split S-1 and actin (Chen et al., 1985). Our findings suggest that one of the conclusions of this study, that there is a difference in the affinity of the 20K and 50K fragments for actin, may be a direct result of the splitting of S-1. The cut between the two actin binding domains could alter the structure of the S-1 such that one of the binding sites moves further from actin. Thus the stoichiometry of the cross-linking product for split S-1 will be lower for the 50K–actin product than for the 20K–actin product. There is no doubt that the angular distribution of probes in the split S-1 decorated rigor fibers is different than that for the native S-1. That this alteration of S-1 affects the 50K actin binding site is a reasonable speculation.

Acknowledgments

We thank J. Belágyi of The Medical University in Pécs, Hungary, for the ESR data and M. F. Morales from UCSF for helpful suggestions.

Registry No. MgADP, 7384-99-8.

References

Ajtai, K., & Burghardt, T. P. (1986) *Biochemistry 25*, 6203–6209.

Borejdo, J., Putnam, S., & Morales, M. F. (1979) *Proc. Natl. Acad. Sci. U.S.A. 76*, 6346–6350.

Borejdo, J., Assulin, O., Ando, T., & Putnam, S. (1982) *J. Mol. Biol. 158*, 391–414.

Botts, J., Muhlrad, A., Takashi, R., & Morales, M. F. (1982) *Biochemistry 21*, 6903–6905.

Burghardt, T. P. (1984) *Biopolymers 23*, 2383–2406.

Burghardt, T. P., & Thompson, N. L. (1984) *Biophys. J. 46*, 729–737.

Burghardt, T. P., & Ajtai, K. (1985) *Proc. Natl. Acad. Sci. U.S.A. 82*, 8478–8482.

Burghardt, T. P., & Thompson, N. L. (1985) *Biophys. J. 48*, 401–409.

Burghardt, T. P., Ando, T., & Borejdo, J. (1983) *Proc. Natl. Acad. Sci. U.S.A. 80*, 7515–7519.

Chen, T., Applegate, D., & Reisler, E. (1985) *Biochemistry 24*, 137–144.
Davydov, A. S. (1963) *Quantum Mechanics*, pp 127–169, NEO Press, Ann Arbor, MI.
Duke, J., Takashi, R., Ue, K., & Morales, M. F. (1976) *Proc. Natl. Acad. Sci. U.S.A. 73*, 302–306.
Hudson, E. N., & Weber, G. (1973) *Biochemistry 12*, 4154–4160.
Mendelson, R., Putnam, S., & Morales, M. F. (1975) *J. Supramol. Struct. 3*, 162–168.
Thomas, D. D., & Cooke, R. (1980) *Biophys. J. 32*, 891–906.
Tonomura, Y., Appel, P., & Morales, M. F. (1966) *Biochemistry 5*, 515–521.
Torgerson, P. M., & Morales, M. F. (1984) *Proc. Natl. Acad. Sci. U.S.A. 81*, 3723–3727.
Weeds, A. G., & Taylor, R. S. (1975) *Nature (London) 257*, 54–56.
Yanagida, T. (1981) *J. Mol. Biol. 146*, 539–560.
Yanagida, T. (1985) *J. Muscle Res. Cell Motil. 6*, 43–52.

Electron Spin Resonance of Calmodulin–Vanadyl Complexes†

Jaime Nieves,‡ Lisa Kim,‡,§ David Puett,§ and Luis Echegoyen*,‡

Departments of Chemistry and Biochemistry and Reproductive Sciences and Endocrinology Laboratories, University of Miami, Miami, Florida 33124

Julio Benabe and Manuel Martinez-Maldonado

Department of Medicine, Veterans Administration Hospital, and University of Puerto Rico School of Medicine, San Juan, Puerto Rico 00936

Received December 12, 1986; Revised Manuscript Received February 19, 1987

ABSTRACT: X-band (9.2 GHz) electron spin resonance spectroscopy was used to investigate the binding of vanadyl to calmodulin. Solution spectra, obtained at ambient temperature with various VO^{2+}:calmodulin molar ratios, suggested a binding stoichioimetry of 4 mol of VO^{2+}/mol of protein and the possibility of two classes of binding sites. The latter was confirmed by using frozen solutions of calmodulin–VO^{2+} complexes that gave splitting of the spectral bands corresponding to the parallel components, which was particularly pronounced with the three high-field peaks. Competition of Ca^{2+} for the VO^{2+} binding sites was investigated, and the results indicated that two of the VO^{2+} sites corresponded to two of the Ca^{2+} sites; the other two VO^{2+} binding sites may have a higher affinity for VO^{2+} than for Ca^{2+} or they may correspond to Ca^{2+}-independent sites. These results demonstrate that electron spin resonance spectroscopy can be used advantageously to probe subtle differences in the microenvironments of metal-binding sites in calmodulin.

Calmodulin is a ubiquitous and multifunctional regulatory protein involved in the regulation of many cellular functions (Cheung, 1980; Means et al., 1982; Klee & Vanaman, 1982). The protein binds four Ca^{2+} ions, two each in globular lobes that are connected by a long central helix (Babu et al., 1985). There is controversy regarding the relative affinities of the four sites, the order of binding, and whether or not cooperativity exists (Haiech et al., 1981; Potter et al., 1983; Burger et al., 1984; Iida & Potter, 1986). ^1H NMR studies are consistent with the presence of two high-affinity binding sites for Ca^{2+} in the carboxy-terminal domain and two low-affinity sites in the amino-terminal domain (Seamon, 1980; Ikura et al., 1983, 1984; Klevit et al., 1984; Thulin et al., 1984). Preferential ordering to Ca^{2+} binding has also been demonstrated by measuring rates of acetylation of the seven lysines in calmodulin; the results were consistent with Ca^{2+} binding first to the carboxy-terminal sites (Giedroc et al., 1987). It is also well recognized that monovalent and divalent metal cations other than Ca^{2+} bind to calmodulin (Forsen et al., 1980; Delville et al., 1980; Haiech et al., 1981; Potter et al., 1983; Cheung, 1984; Shimizu & Hatano, 1984; Wang et al., 1984; Mulqueen et al., 1985; Mills & Johnson, 1985).

Vanadium is an essential trace metal in experimental animals (Schwarz & Milne, 1971), and it is known that vanadate is rapidly and quantitatively converted to vanadyl (VO^{2+}) by glutathione and catechols (Cantley et al., 1978; Macara et al., 1980). Thus, VO^{2+} may have physiological significance. This cation forms strong complexes with a variety of ligands and binds to numerous metalloproteins (Chasteen, 1981, 1983); this ability to bind to diverse proteins may arise from the flexibility in the coordination geometry of VO^{2+} (Chasteen, 1981). In a preliminary paper we showed that VO^{2+} binds to calmodulin (Ahmed et al., 1985); herein we present ESR spectral data suggesting that VO^{2+} binds to the protein with a stoichiometry of 4:1 and demonstrate the existence of two classes of binding sites.

Materials and Methods

Materials. HEPES,[1] calcium chloride, and vanadyl sulfate were obtained from Sigma Chemical Co. (St. Louis, MO). Calmodulin was purified to homogeneity from bovine testes as described elsewhere (Jackson & Puett, 1984); special care

† This research was supported by Research Grant GM35415 from the National Institutes of Health.
‡ Department of Chemistry.
§ Department of Biochemistry and the Reproductive Sciences and Endocrinology Laboratories.

[1] Abbreviations: HEPES, *N*-(2-hydroxyethyl)piperazine-*N*′-2-ethanesulfonic acid; DPPH, diphenylpicrylhydrazyl.

0006-2960/87/0426-4523$01.50/0